eJSE International

Electronic Journal of Structural Engineering 22 (3) 2022

Nonlinear Finite Element Analysis of Bonding Behavior of Corroded Mortar Anchor under Dynamic Load

Haitao Wang [a, *], Minghua Cui [a], Kun Ren [a], Haoyu Sun [a]

[a] *School of Civil Engineering, Dalian Jiaotong University, Dalian, China*

[*] *Corresponding Author, E-Mail: whtdjtu@163.com*

ABSTRACT: The connection between reinforcement and mortar was established through the surface-to-surface contact method. The transient dynamic Full method was adopted for dynamic loading solution. The numerical analysis model for the bonding performance of corroded mortar bolts under dynamic load was established. The numerical analysis results were compared with the test results for verification. The bond properties of the anchorage interface under the conditions of different mortar protection thickness, anchorage length and corrosion rate were analyzed. The results show that the numerical simulation results are in good agreement with the test results. The numerical model can analyze the bonding performance of the corroded mortar bolts. Within a certain limit, the bond stress is positively correlated with the thickness of the mortar protective layer. The larger the anchorage length is, the greater the bonding stress at the loading end will be, and the more uneven the distribution of bonding stress in the anchorage segment will be. However, when the anchorage length reaches a certain value, the continuous increase of anchorage length will have no obvious effect on the improvement of its bonding performance, so there is an optimal anchorage length. With the increase of the corrosion ratio, the bonding stress peak decreased gradually.

KEYWORDS: Dynamic loading; Corroded mortar bolt; Bonding performance; Parameter analysis

1 INRODUCTION

In recent years, with the rapid development of computer technology and various kinds of finite element software, finite element simulation technology has been applied more and more in practical engineering. It has become a powerful tool for the research of various problems in various kinds of anchorage structures. Although various scholars have different research methods, their research has important reference value for in-depth analysis of anchoring mechanism and related parameter research, and many achievements have been obtained (Ge and Li，2008). The finite element numerical simulation method is also widely used in the classical pull-out test of anchoring bond. Jiang et al. (2008) established a finite element model based on the constitutive relation of Mohr-Coulomb's elastic-perfectly plastic theory by using the three-dimensional explicit finite difference method. Liu et al. (2009) fitted the field test data according to the hyperbolic model of the interface spring theory. They made corresponding modeling analysis by using the spring element Combin39 in the finite element analysis software ANSYS. Yu et al. (2016) conducted a nonlinear finite element analysis on the test based on the reinforcement drawing test by using the large general finite element program ANSYS. They studied the influence of different loads and anchorage lengths on the bond stress distribution, and then compared and verified the finite element analysis results with the test results. Deb et al. (2011) defined solid elements that intersect with the anchor rod in any direction as "enrichment " elements and had additional degrees of freedom at each node to estimate the displacement and stress in the bolt. Based on this enrichment finite element method (EFEM), the mechanical properties of rock reinforced by grouting bolt were analyzed.

In other related research of anchoring bond, more achievements have been made through finite element software simulation. Zhan et al. (2006) adopted the nonlinear finite element method and Coulomb yield criterion to simulate anchor rod and grouting body by solid element. They simplified the numerical calculation model to axisymmetrical problem and studied the shear stress distribution along bolt under different loads and the influence of rock and soil properties under reinforcement on it. Degger et al. (1995) analyzed the failure mechanism of volume expansion caused by corrosion products in concrete structures though numerical simulation method. Based on the existing crushing fracture model, a two-dimensional linear finite element program for cracking of corroded concrete was developed, which provided an idea for understanding the damage propagation mechanism of concrete structure delamination and spalling caused by steel corrosion. Zhang et al. (2001) proposed a simulation method that used temperature expansion ring instead of volume expansion of corrosion products to solve the problem of steel rust expansion in concrete. Different corrosion conditions can be simulated by changing different parameters of temperature

expansion ring. Li (2018) conducted finite element numerical simulation using ABAQUS software on the basis of the drawing test, simulated the bond between reinforcement and concrete through the Spring2 nonlinear spring element, and considered the influence of dynamic load (loading rate) on the mechanical properties of specimens during the modeling process.

The corrosion of the bolt affects its anchoring effect and the safety of the whole project. At the same time, dynamic loads, including seismic loads, pose a greater threat to in-service corroded bolts. Therefore, the research on the bond behavior and mechanical response of the bolt under the coupling effect of dynamic load and corrosion is helpful to the safety evaluation of the existing bolt supporting system and has important practical significance for the evaluation of the anchorage capacity of the bolt and the reinforcement and maintenance scheme.

In order to study the bonding property of the interface between corroded rod body and grouting body, the characteristic parameters and constitutive relations of the two materials should be determined first when establishing the finite element model. However, there are few research on the constitutive relation of corroded mortar bolt. Therefore, by referring to relatively mature research methods and relevant parameters of reinforced concrete (Duan,2014; Xia,2005; Hong,2000), this paper chose to establish a solid model of reinforcement, and studies the interfacial bond behavior through the surface-to-surface contact analysis function in ANSYS software. Due to the research state is dynamic, this simulation is based on transient dynamics theory and adopt the transient loading mode provided by software at the same time.

2 THE ESTABLISHMENT OF NUMERICAL ANALYSIS MODEL

2.1 *Selection of parameters in the numerical model*

2.1.1 *Reinforcement*

The elastic-perfectly plastic model can be used for the constitutive model of reinforcement, and the elastic-plastic model with strengthened stage can also be used for the aid of convergence. In this paper, BISO (Bilinear isotropic) was adopted to simulate. The constitutive model curve was obtained by automatically providing the stress-strain data table through the program of inputting the yield strength of reinforcement (300MPa in this simulation).

2.1.2 *Mortar*

Mortar is a kind of granular material; its tensile strength is much greater than compressive strength. When the material is under shear, the particles will expand to a certain extent. Drucker-prager yield criterion can be used to describe the yield performance of such materials. The yield surface of this criterion do not change with the gradual yield of materials, but its yield strength increase with the increase of lateral confining pressure. The constitutive model adopted ideal elastic-plastic. This material option is suitable for granular materials such as concrete, rock and soil. The material properties of DP material were input through the data table in the program, and the following three material parameters needed to be input: cohesion C1, internal friction angle C2 and dilation angle C3. The dilation angle is used to reflect the size of control material volume expansion. When the dilation angle is equal to the friction angle, the volume will expand seriously. When the dilation angle is 0 or less than the friction angle, the volume will not expand or slightly expand. It is more conservative to set the dilation angle at 0. The dilation angle was 0 in this paper.

The relevant parameters of each material in this simulation are shown in Table 1.

Table 1. Material parameters of the model.

Material type	Elastic modulus (MPa)	Poisson ratio	Cohesion (MPa)	Internal friction angle (°)
Mortar	2.1×10^4	0.3	1.5	25
Reinforcement	2.0×10^5	0.27	-	-

2.1.3 *Parameter selection of corrosion simulation*

The friction coefficient MU is an important parameter in the contact unit, which directly reflects the roughness of the contact surface. In this simulation, the change of the friction coefficient reflected the corrosion of the reinforcement. Based on the measured test data and relevant research experience, ANSYS was used for inversion. A large number of trial calculations in the early stage showed that when the friction coefficient of the rust-free part was set as 1.0, and the friction coefficient of the rust corroded part was set as 0.53, the numerical simulation results were most similar to the test results. Therefore, the friction coefficient MU of the rust-free parts and the rust-corroded parts was set as 1.0 and 0.53 respectively in this numerical simulation.

In the initial loading process, the slip between the reinforcement and the grout is small, so the bond stress mainly depends on the chemical adhesive force, and the compressive stress of the reinforced-mortar interface have little influence on the bond stress. Therefore, we know that the initial cohesion value is the

bond stress when the amount of slip is small. When the slip is 0.2mm, the bond stress is taken as the initial cohesion value c0. For example, when the loading frequency of uniform corrosion specimens is 1Hz, the initial cohesive force is 7.8MPa.

2.2 *The establishment of finite element model*

2.2.1 *Mesh subdivision and constraints*

A separate model was used in this paper. In most relevant studies, in order to reduce the finite element solution scale and calculation time, researchers simplify the specimen to a quarter model for calculation and solution according to the symmetry of the specimen. However, most of the previous studies were under the condition of static load, while the load applied in this paper was sinusoidal load, which did not have the condition of symmetry treatment. Therefore, the complete finite element model was still established according to the actual size of the drawing test specimen. The volume mapping partition method was adopted to divide the grid, as shown in Fig.1.In the actual test, the counterforce frame was used for pull-out test, so the longitudinal freedom of all nodes on the mortar surface at the loading end was constrained in the model, and the tensile force was applied to the reinforcement end face at the loading end.

SOLID65 unit was adopted to simulate mortar, which has eight nodes and each node had three degrees of freedom, namely, linear displacement in x, y and z directions. SOLID65 unit is specially developed for heterogeneity materials such as concrete and rock, its compressive strength is much higher than that of tensile strength. It can simulate reinforced rib in concrete and phenomena such as tensile crack and crushing of materials, etc. It has the ability of cracking, crushing, flowing deformation and time-yield. Solid unit SOLID185 was adopted to simulate reinforcement. The element has eight nodes, and each node had three translational degrees of freedom along the x, y and z directions. It has super elasticity, stress tempering, creep, large deformation and large strain capacity, which is suitable for simulating incompressible elastic-plastic materials like reinforcement. It has the characteristics of hyper elasticity, stress tempering, creep, large deformation and large strain capacity, so it is suitable to simulate almost incompressible elastic-plastic materials such as reinforcement.

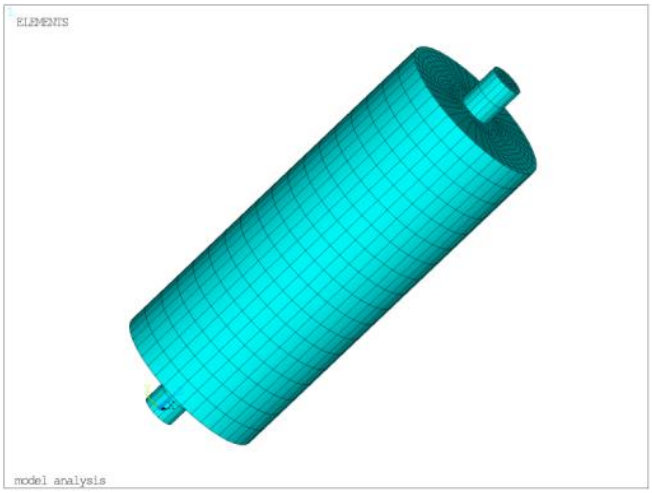

Figure 1. Finite element meshing of the model.

The key point of this simulation is the bond slip between reinforcement and mortar. At present, in most of the bond slip simulations, two-dimensional bar element is selected to simulate the reinforcement. The reinforcement is simplified as a line. The nonlinear spring element COMBIN39 is used to realize the connection of reinforcement and encased concrete. Although this simplification is convenient for modeling and operation, it cannot simulate the actual situation of reinforcement and contact surface. At the same time, the COMBIN39 unit cannot simulate plasticity, creep, large strain and initial stress, etc. Therefore, in this modeling, solid unit was selected to establish the model of actual size reinforcement, and zero-thickness surface-to-surface contact unit was adopted to simulate the bonding situation between reinforcement and mortar. Reinforcement was selected as the target surface and mortar as the contact surface, TARGE170 as the target unit and CONTAC173 as the contact unit.

In the process of pull-out test, concrete is poured around the rock bolt to simulate the action of surrounding rock, and the research focus of this paper was on the bond performance between reinforcement and mortar. Therefore, in order to improve the simulation efficiency in the numerical simulation process, only the reinforcement and mortar models were established, and a constraint load was applied on the periphery of the cylindrical mortar to simulate the surrounding rock effect. According to previous studies and many trial calculations, the initial stress of surrounding rock is 2.83MPa. As the confining pressure also restricts the axial displacement of the outer surface of the bolt, the normal constraint was applied only on the outer surface.

2.2.2 *Loading and solving*

The complete transient dynamic analysis was used in the simulation. Because the pull-out load was the sine load increasing step by step, the function relation of

sine load in each stage was defined by function tool in ANSYS and saved in the software. When the load was applied at the pull-out end, the sine load of each section was called as multi load step loading through table load (formed by software automatic transformation). And load step was written into LS file. Fig. 2 shows the sine load under the first stage load (10kN) when the loading frequency of the writing software was 1Hz, and the other levels of load are likewise.

For the non-linear analysis of ANSYS, the parameter setting is also very important. A lot of trial calculations are needed in the early stage to select the appropriate parameters to ensure the convergence and accuracy of the calculation. In the process of this solution, the automatic time step was activated, and the upper and lower limits of integration step were specified by DELTIM and NSUBST to relax the convergence tolerance.

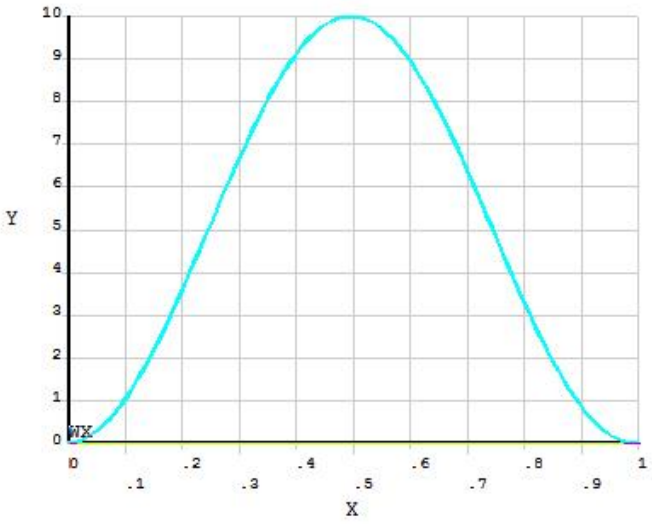

Figure 2. Sine load setting.

3 DYNAMIC BOND PERFORMANCE ANALYSIS OF CORRODED MORTAR ANCHOR

3.1 *Experimental study on dynamic bonding performance of corroded mortar anchor*

In order to study the influence of corrosion action, corrosion position and loading frequency on the interfacial bonding performance of mortar anchor, orthogonal tests were designed as shown in Table 2. The anchorage length of all specimens in the control group was 180mm.

Table 2. Pull-out test conditions of anchorage body.

Specimen group	Specimen number	Corrosion location	Loading frequency/ Hz
A	S1	No corrosion	0.1
	S2		0.5
	S3		1.0
	S4		2.0
B	S5	Uniform corrosion	0.1
	S6		0.5
	S7		1.0
	S8		2.0
C	S9	Front corrosion	0.1
	S10		0.5
	S11		1.0
	S12		2.0
D	S13	Middle corrosion	0.1
	S14		0.5
	S15		1.0
	S16		2.0
E	S17	Posterior corrosion	0.1
	S18		0.5
	S19		1.0
	S20		2.0

The test model was designed according to the structural characteristics of the anchor in the actual project. The rod body was threaded reinforcement, the grouting body was cylindrical mortar, and the circular ring concrete was used to simulate the outer surrounding rock. The reinforcement adopts the hot rolled crescent shaped reinforcement with diameter of 16mm and yield strength of 335MPa. The relative protective layer of the specimen was taken as $c/d=4.5$ (c: the thickness of mortar and concrete protective layer, d: the diameter of reinforcement), and the enclosing layer of reinforcement was 29.5mm mortar layer and 42.5mm concrete layer, respectively. The overall diameter of the specimen was 160mm. Considering the local extrusion effect of the bearing steel plate on the loading end during the loading process, 50mm unbonded sections were set at the loading end and free end of the anchor respectively, and the reinforcement was separated from the mortar through the PVC sleeve with an inner diameter of 20mm to ensure that there was no bonding between the mortar at the end and the reinforcement. In order to obtain more accurate strain of reinforcement in the process of pull-out test and not to destroy the bond between reinforcement and mortar, we stuck the strain gauge in the groove of reinforcement is adopted.

Considering the particularity of this study -- to conduct subsection corrosion on part of the reinforcement, in order to control the corrosion position accurately, the reinforcement should be corroded first and then grouting. The corrosion scheme was as follows: normal treatment shall be carried out for the reinforcement without corrosion or uniform corrosion;

special anti-rust treatment shall be carried out at some positions for the reinforcement with different corrosion positions -- wrapped the non-rust part with insulating tape, wrapped the anchor section and strain gauge wire with water pipe, and then conduct wet electrification corrosion. Based on the Faraday's law, the design corrosion can be controlled by calculation according to the design electrification time and current intensity. The designed corrosion rate of all specimens in the test was 3%.

The MTS electro-hydraulic servo test system (810 Material Test System) was used to control the loading frequency of the pull-out test. The sinusoidal loading scheme contained four different frequency. Through the computer digital controller, the loading waveform and parameters required by the test were set. At the same time, load, displacement and other test data was recorded in real time during the loading process. DH3817 dynamic-static strain test and analysis system was used in the test to collect the reinforcement strain in the loading process in Fig. 3.

Figure 3. DH3817 dynamic-static strain test and analysis system.

In order to facilitate the wiring of the strain collection system and fix the specimen better, the loading device was customized according to the size of the processing. The device was composed of two steel plates at the top and the bottom and four high-strength steel rebar at the four corners. The steel plate and steel bar were assembled by matching nuts, and the height of the loading device can be adjusted according to the length of the specimen. Pass the reinforcement through the reserved circular hole in the center of the lower steel plate, and place the specimen in the loading device. The ball hinge pull rod on the upper steel plate of the loading device was fixed by the upper chuck of MTS testing system, and the steel bar exposed from the hole of the lower bottom plate was clamped by the lower chuck, as shown in Fig. 4. After the loading system was started, the upper part of the loading device was fixed by the testing machine, and the lower chuck of the testing machine controls the vertical reciprocating movement of the specimen through the sinusoidal load set, so that the reinforcement was gradually pulled out.

Figure 4. Schematic diagram of pull-out test.

Based on the reinforcement strain of each specimen, the bond stress distribution curve was fitted, as shown in Fig. 5. The results showed that: with the increase of the peak load at all levels, the bond stress at the loading end increased faster, the bond stress peak increased gradually, and the bond stress transferred to the free end continuously. The peak value of the bond stress of the corroded specimen was smaller than that of the rust-free specimen, and the peak value of the bond stress of the rust-free specimen was 20.6MPa. In the process of unloading, the sinusoidal cyclic loading had a reverse bonding stress, and the distribution of the bonding stress showed a "double peak" trend, but this trend was not obvious in the corrosion specimens. The distribution of bond stress with different corrosion positions of reinforcement was different. The peak of bond stress did not appear in the corrosion area at the anchorage section. The peak value of the bond stress of the specimen with the front corrosion of reinforcement was the smallest, which was only 18.03MPa. Therefore, in order to ensure the effective bond length, the anchoring quality of the front of the anchorage section (loading end) was very important. With the increase of loading frequency, the bond stress increases faster and the bond stress peak increases. When the loading frequency is 2Hz, the bond stress peak reached 21.2MPa, and the bond stress transferred distance along the direction of anchorage was shorter.

3.2 *Comparative analysis of numerical simulation results and experimental results*

The post processor（Post1） was used to analysis the contact compressive stress of each node along the anchorage direction of the bond interface. The bond stress at each point was calculated by Coulomb formula, and the distribution curve of the bond stress along the anchorage length was drawn.

3.3 *Comparison of ultimate bond stress calculation results*

The corresponding finite element analysis was carried out on 20 specimens, and the analysis results of the ultimate bonding stress of each specimen were extracted and compared with the test results, as shown in Table 3. It can be seen from the table that the ultimate bonding stress obtained by numerical simulation was quite consistent with the test results, with an average error of 4.1%, indicating that the numerical simulation method proposed was feasible. It can carry out a large degree of reduction simulation for the pull-out test.

Table 3. Comparison of numerical simulation and experimental results of ultimate bond stress.

Specimen number	Test value/MPa	Analog value/MPa	Error/ %
S1	20.66	19.87	3.98
S2	20.92	20.39	2.60
S3	21.79	20.47	6.45
S4	22.41	24.28	8.34
S5	16.56	17.34	4.71
S6	17.28	16.63	3.91
S7	18.63	17.62	5.73
S8	20.45	19.57	4.50
S9	17.03	17.51	2.82
S10	17.96	18.19	1.28
S11	18.35	17.46	5.10
S12	18.92	18.27	3.56
S13	18.47	18.16	1.71
S14	19.26	18.13	6.23
S15	19.73	19.32	2.12
S16	20.06	20.79	3.64
S17	17.82	17.06	4.45
S18	19.94	19.77	0.86
S19	20.21	20.84	3.12
S20	20.93	19.57	6.95

3.3.1 *Comparison of bond stress distribution*

Fig. 5 (a) to Fig. 5 (e) compare the numerical simulation results and test results of the bond stress of some specimens under various peak loads with the loading frequency of 1Hz. It can be seen from the figure that the characteristics of the bond stress distribution curve calculated by the finite element method were quite consistent with the test results, but the numerical simulation results still had some differences with the test results in terms of the peak value and position of bond stress, local bond stress and so on. This was mainly reflected in the fact that the simulated value of the bond stress at the loading end was slightly larger than the experimental value, the peak value of the bond stress appeared slightly forward, and the curve distribution of the simulated result of the bond stress was smoother and even. These differences were mainly caused by the modeling method. The simplification of replacing twisted steel bars with plain steel bars bar will lead to certain deviation in the results. In addition, there were many coupling factors in the actual physical test, and the finite element modeling was an ideal analysis, so there will be some errors between the results. However, these differences were still within the acceptable range, so the finite element analysis of physical drawing test with ANSYS was feasible.

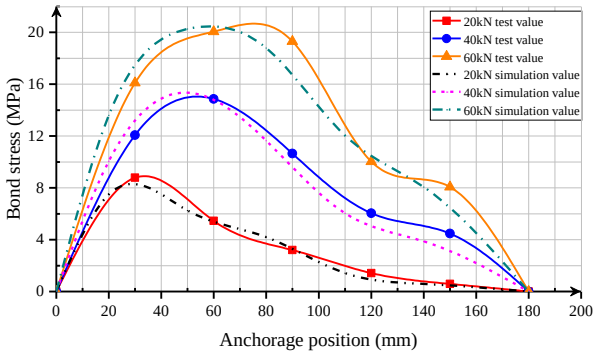

(a) No corrosion (specimen S3)

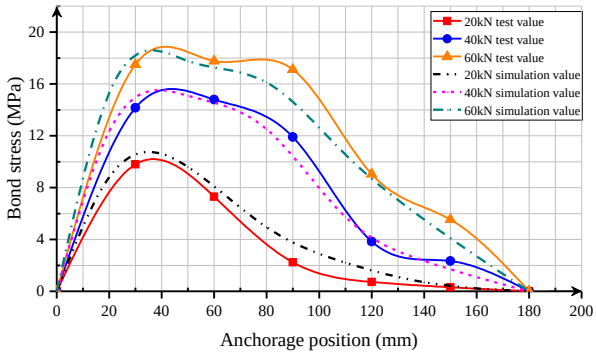

(b) Uniform corrosion (specimen S7)

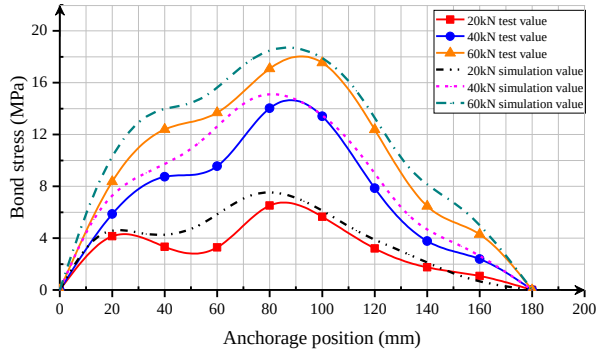

(c) Front corrosion (specimen S11)

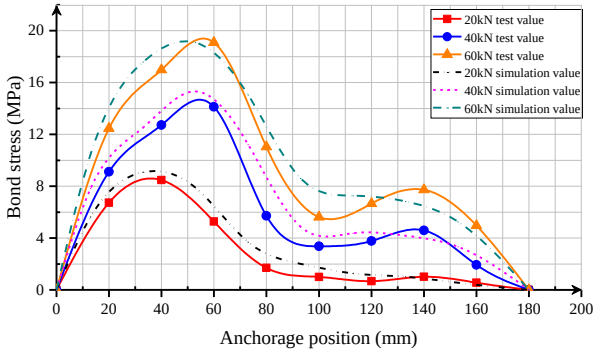

(d) Middle corrosion (specimen S15).

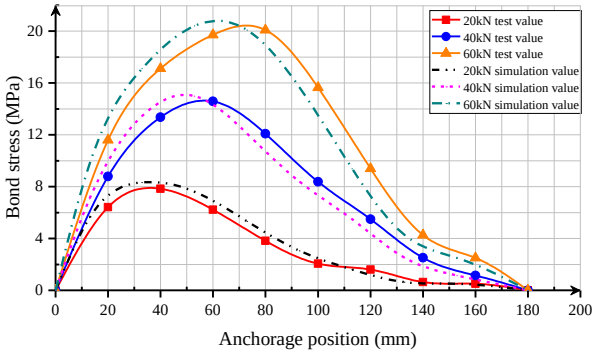

(e) Posterior corrosion (specimen S9).

Figure 5. Comparison of numerical simulation results and experimental results of bond stress curves.

4 SENSITIVITY ANALYSIS OF ANCHORAGE INTERFACE BOND PERFORMANCE PARAMETERS

Through the comparative analysis of the numerical simulation results, it can be known that ANSYS finite element analysis can be used to carry out a good simulation of the anchor rod pull-out test, and more reliable results were obtained. The application of numerical simulation can make up for the shortage of long period and high cost of physical test to a certain extent, and break the limitation of test conditions. Based on the above finite element calculation, several groups of numerical simulation of orthogonal test were carried out to study the influence of mortar cover thickness, anchorage length and corrosion rate on the bond performance of anchorage interface.

4.1 *Analysis of the influence of mortar cover thickness on bonding performance*

The existence of mortar layer had an important influence on the mechanical properties of anchor rod. Specimen S1 was selected as the basic model to study the influence of mortar protective layer thickness on bonding performance. The mortar protective layer thickness of 4 models were 19.5mm, 59.5mm, 89.5mm and 119.5mm respectively. Except for the difference of mortar mesh division, the other parameter values and simulation ideas were the same as S1. According to the calculation results with peak load of 50kN, the distribution diagram of bond stress and ultimate bond stress value under different protective layer thickness are drawn in Fig. 6 and Fig. 7. It can be seen from the figures that, under the same load, the greater the thickness of the mortar protective layer, the greater the bonding stress. This is because with the increase of the thickness of the mortar protective layer, the restraint effect of the protective layer on the reinforcement becomes larger, which improves the overall friction force between the reinforcement and the mortar to a certain extent, so the bonding stress of the anchorage interface increases accordingly.

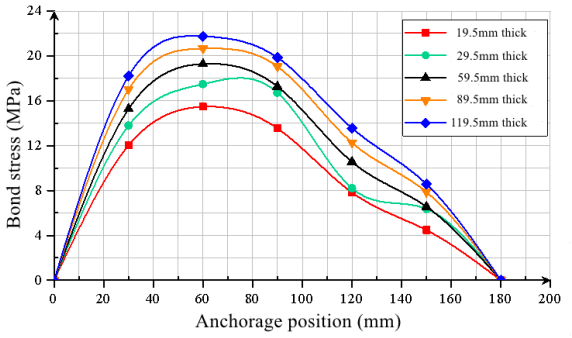

Figure 6. Bond stress distribution under different mortar thickness.

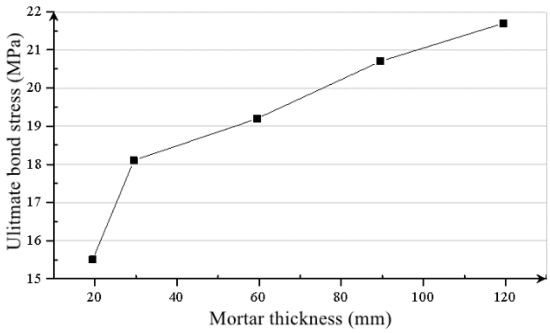

Figure 7. Effect of the mortar thickness on the ultimate bond stress.

4.2 4.2 *Analysis of the influence of anchorage length on bonding performance*

In order to study the influence of anchorage length on bonding performance, specimen S1 was selected as the basic model of numerical simulation. The anchorage length of the other 3 models were 240mm, 300mm and 360mm. Except for the difference of reinforcement mesh division, the other parameter values and simulation ideas were the same as S1. The variation curve of bond stress along the direction of anchorage is drawn in Fig. 8. It was based on the calculation results under the extracted peak load of 40kN. It can be seen from the figure that, under the same load, the peak value of the bonding stress curve gradually increased and moved towards the loading end as the anchorage length increases. The

larger the anchorage length, the greater the bonding stress at the loading end, and the more uneven the bonding stress distribution in the anchorage section. This result also verified the conclusions of many studies: the force of the rod was mainly concentrated in the front of the rod, and the longer the anchorage length, the more obvious the phenomenon. In combination with Fig. 9, it can also be inferred that an appropriate increase in the anchorage length was helpful to improve the bond stress. When the anchorage length reached a certain value, there will be no obvious effect on the improvement of the mechanical properties of the anchor if the anchorage length continues to increase.

(a) Anchorage length 180mm.

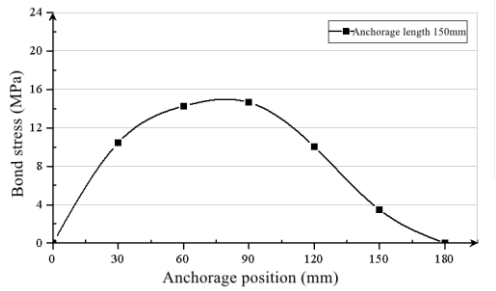

(b) Anchorage length 240mm.

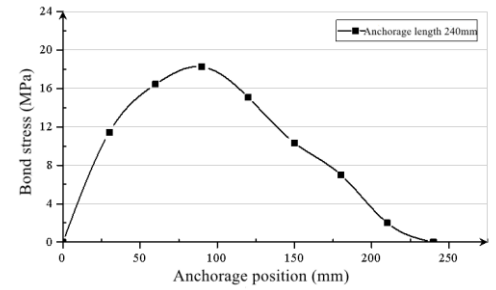

(c) Anchorage length 300mm.

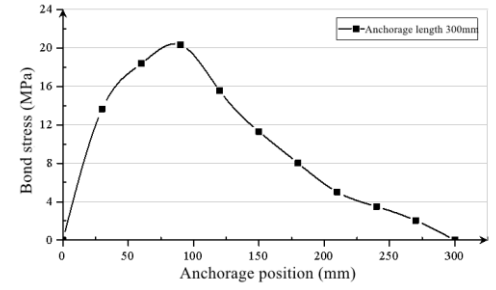

(d) Anchorage length 360mm.

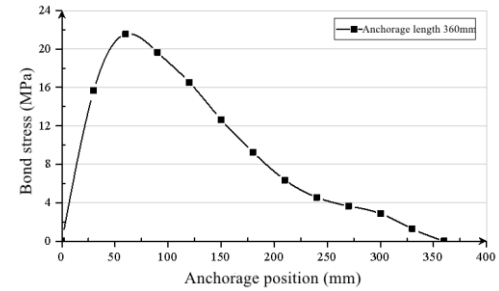

Figure 8. Bond stress distribution under different anchorage lengths.

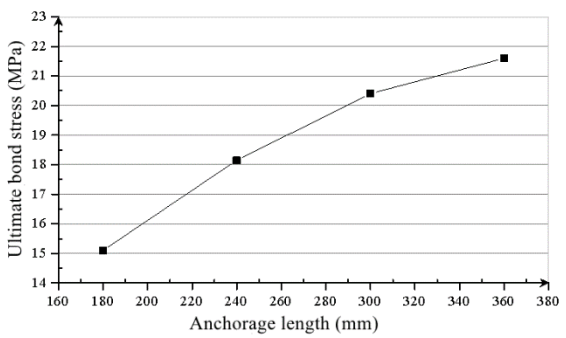

Figure 9. Effect of anchorage length on ultimate bond stress.

4.3 *Analysis of the influence of corrosion rate on bonding performance*

On the basis of 3% corrosion ratio, in order to study the influence of corrosion ratio on the bond performance, the S5 specimen was used as the basic model in the numerical simulation, and three models with corrosion rates of 2%, 5% and 7% were added. Based on relevant research experience and model trial calculation, the corresponding friction coefficient MU was respectively 0.59, 0.31 and 0.18 to simulate the situation of contact surface. The variation curve of bond stress along the direction of anchorage and the distribution diagram of ultimate bond stress are drawn in Fig. 10 and Fig. 11 based on the calculation results under 50kN peak load extracted. It can be seen from the figures that under the same load peak value, with the increase of corrosion ratio, the peak value of bond stress decreases obviously. The distribution of bond stress along the direction of anchorage length was more uniform. It is because that the mechanical bite between reinforcement ribs and mortar gradually weakens, and the chemical adhesive force between reinforcement and mortar was also damaged with the increase of corrosion products. This makes the load more easily transferred in the anchorage section, so the bond stress distribution was more uniform.

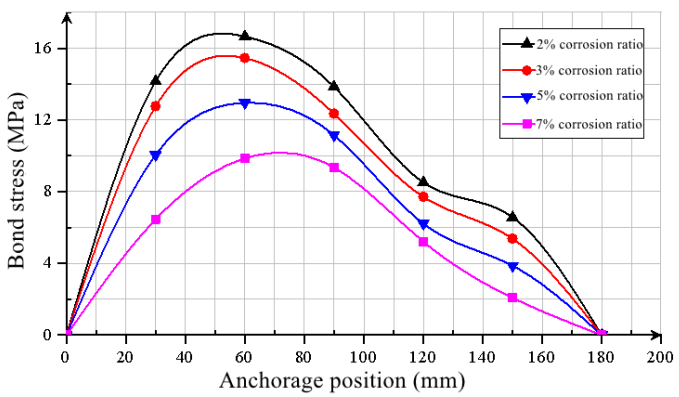

Figure 10. Bond stress distribution under different ratios of corrosion.

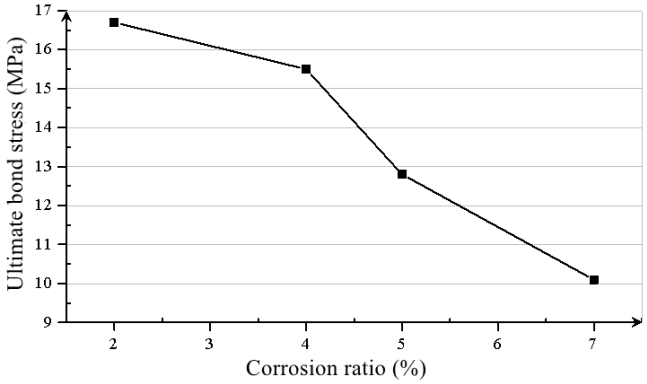

Figure 11. Effect of corrosion ratio on ultimate bond stress.

5 CONCLUSION

The connection between reinforcement and mortar was established by plane-plane contact, and the dynamic loading was solved by transient dynamic Full method. The numerical analysis model of the bonding performance of corroded mortar bolts under dynamic load was established, and the results of the numerical analysis were compared with the test results for verification. At the same time, the bond properties of the anchorage interface under the conditions of different mortar protection thickness, anchorage length and corrosion rate were analyzed. The following conclusions were drawn:

(1) The numerical simulation results were in good agreement with the test results, indicated that the numerical model can better analyze the bonding performance of the corroded mortar bolt. The finite element analysis of the physical drawing test with ANSYS was feasible.

(2) Parameter sensitivity analysis results show that: within a certain limit, the greater the thickness of mortar protective layer, the greater the bond stress. The larger the anchorage length was, the greater the bonding stress at the loading end would be, and the more uneven the distribution of bonding stress in the anchorage segment would be. However, when the anchorage length reached a certain length, the further increase will have no obvious effect on improving the bonding performance of the anchor rod, so there was an optimal anchorage length. The higher the corrosion rate, the smaller the bonding stress peak, and the more uniform the bonding stress distribution along the anchorage length direction.

6 ACKNOWLEDGEMENT

This work was supported by the Foundation for Dalian Distinguished Young Scholars under grant [number 2018RJ10]; the Project supported by the Natural Science Foundation of Liaoning province, China under grant [number 2020-MS-271]; and the Program Funded by Liaoning Province Education Administration under grant [number JDL2020010].

7 AUTHORS' CONTRIBUTIONS

Author 1: (First Author, Corresponding Author): Conceptualization, Methodology, Formal Analysis, Writing - Original Draft, Funding Acquisition, Resources.
Author 2: Data Curation, Software, Writing - Original Draft.
Author 3: Visualization, Investigation, Validation.
Author 4: Resources, Investigation, Supervision.

8 DECLARATION OF INTEREST STATEMENT

The authors declare that they have no known competing financial interests or personal relationships that could have appeared to influence the work reported in this paper.

9 REFERENCES

Duan G.T. “Corrosion medium diffusion model of mortar bolt and numerical test study of drawing”. Dissertation, Chongqing University, 2014.

Deb D, Das K.C. “Modelling of fully grouted rock bolt based on enriched finite element method”. International Journal of Rock Mechanics & Mining Sciences, 2011, Vol. 48, No. 2, pp. 283-293.

Degher H.J., Kulendran S. “Finite element modeling of corrosion damage in concrete structures”. ACI Structure Journal, 1995, Vol. 89, No. 6, pp. 1179-1190.

Ge W.J., Li X.B. (2008) “Application of numerical simulation in bolt support technology”. Pneumatic tools for rock drilling machinery, 2008, No. 1, pp. 131-34.

Hong X.J., Zhang Y. “Fitting method of bond stress in bond slip test”. Structural Engineer, 2000, No. 3, pp. 44-48.

Jiang W.W., Xu G.Y., Ma C.N. “Application of fast Lagrangian method in numerical simulation test of bolt drawing”. China Railway Science, 2008, Vol. 29, No. 6, pp. 50-54.

Li G.Y. “Numerical simulation of dynamic bond performance of reinforced concrete”. Dissertation, Dalian Ocean University, 2018.

Liu B., Li D.Y. “Test fitting analysis and simulation of the bond-slip relationship of bolt mortar”. Journal of Hefei University of Technology (Natural Science Edition), 2009, Vol. 32, No. 10, pp. 60-63.

Xia N. “A preliminary study on the mechanical properties and durability evaluation of corroded anchors”. Dissertation, Hohai University, 2005.

Yu Q., Yuan W.H., You G.S. “Experimental study and finite element analysis of the bond performance between ribbed steel bars and grouting material”. Structural Engineer, 2016, Vol. 32, No. 6, pp. 113-122.

Zhan Y.B., Bi X.K., You C.A., Lu X.L., Sun F. “Numerical simulation analysis of anchorage stress distribution law”. Rock and Soil Mechanics, 2006, Vol. 27, No. S2, pp. 935-938. https://doi.org/10.16285/j.rsm.2006.s2.003

Zhang W.P., Zhang Y. “Computer simulation analysis of the corrosion expansion process of steel bars in concrete”. Journal of Tongji University (Natural Science Edition), 2001, Vol. 29, No. 11, pp. 1374-1377.